

Article

A Method to Reduce Eddy Current Loss of Underwater Wireless Power Transmission by Current Control

Jiale Wang ^{1,*}, Baowei Song ² and Yushan Wang ¹ 

¹ School of Marine Science and Technology, Northwestern Polytechnical University, Xi'an 710072, China; yushanwang@mail.nwpu.edu.cn

² Key Laboratory for Unmanned Underwater Vehicle, Northwestern Polytechnical University, Xi'an 710072, China; songbaowei@nwpu.edu.cn

* Correspondence: 2015wj1650@mail.nwpu.edu.cn; Tel.: +86-151-2928-7281

Abstract: In recent years, wireless power transmission (WPT) technology based on magnetic resonance has been extensively studied. However, in contrast to that in the air, wireless power transmission in seawater medium will be accompanied by inevitable energy loss, that is, eddy current loss (ECL), which will increase with the frequency and coil current. In this article, an equivalent circuit model of the eddy current loss of underwater wireless power transmission is established, two methods to reduce the eddy current loss are proposed, and the optimal modulus ratio for the coil current of the dual-coil wireless power transmission system to reduce eddy current loss is calculated. Electromagnetic field (EMF) simulation software verifies the correctness of the two methods, and it is concluded that increasing the phase difference of the coil current or controlling the coil current ratio to ensure that the optimal modulus ratio is in a certain range can reduce the eddy current loss effectively and improve the energy transmission efficiency of the system by about 4~5%.

Keywords: wireless power transmission (WPT); current control; eddy current loss (ECL); electromagnetic field (EMF)



Citation: Wang, J.; Song, B.; Wang, Y. A Method to Reduce Eddy Current Loss of Underwater Wireless Power Transmission by Current Control. *Appl. Sci.* **2022**, *12*, 2435. <https://doi.org/10.3390/app12052435>

Academic Editor: Subhas Mukhopadhyay

Received: 11 January 2022

Accepted: 24 February 2022

Published: 25 February 2022

Publisher's Note: MDPI stays neutral with regard to jurisdictional claims in published maps and institutional affiliations.



Copyright: © 2022 by the authors. Licensee MDPI, Basel, Switzerland. This article is an open access article distributed under the terms and conditions of the Creative Commons Attribution (CC BY) license (<https://creativecommons.org/licenses/by/4.0/>).

1. Introduction

Wireless power transmission (WPT) technology through magnetic resonant has been widely studied in recent years because of the number of advantages it has compared with traditional power delivery, such as the convenience of its nonphysical connection between the power supply and the load [1–4]. Especially in the underwater environment, WPT technology solves the problem of wet plugging and the unplugging of underwater energy supply and provides a safer method for the rapid charging of autonomous underwater vehicles (AUVs) [5–8] and unmanned underwater vehicles (UUVs). Therefore, in view of the widespread application of underwater WPT technology, it is of great research significance to improve its energy transmission efficiency.

The WPT system in the air uses one or more pairs of induction coils. The alternating current (AC) of the primary-side coil generates the induced alternating current (AC) in the coupled secondary-side coil, and then the direct current (DC) is generated through rectification to complete the power supply to the equipment. The process of underwater WPT is similar to that in the air, but the medium in the transmission area changes from air to seawater. Therefore, the coupling characteristics between the coils have changed, and the changed magnetic field will generate eddy current in the seawater, which brings new energy loss, namely, eddy current loss. Shi et al. [9] analyzed various losses in underwater WPT systems, including copper loss, semiconductor loss, core loss, and eddy current loss by using circuit analysis and electromagnetic field (EMF) simulation. This article studies the method of reducing eddy current loss to improve the energy transmission efficiency of underwater WPT systems.

In order to reduce the eddy current loss of underwater WPT systems, several researchers have studied it. Zhang et al. [10] analyzed some factors that affect the eddy current loss of underwater charging systems, and used EMF simulation software to optimize the number of coil turns on the primary side and the secondary side and the frequency of the AC source, thereby reducing the eddy current loss, and also designed experiments to verify optimization results. Zhang et al. [11] presented a new coil structure, taking advantage of two primary-side coils placed symmetrically adjacent to each side of the secondary-side coil to reduce the eddy current loss of WPT systems for underwater vehicles. Additionally, their experimental results show that the method improves the energy transmission efficiency of the system significantly by nearly 10%. Yan et al. [12] established the analytical model of the eddy current loss of the coreless WPT system in seawater. Additionally, the expression of the eddy current loss was deduced. They analyzed the eddy current loss under different conditions and concluded that the effect of eddy current loss in seawater would shift the optimal resonance frequency of the system compared to in the air. Moreover, they calculated the optimal resonance frequency according to the analytical model so as to reduce the eddy current loss and improve the energy transmission efficiency of the system. Kim et al. [13] used Z-parameters to analyze the characteristics of eddy current loss and power transfer efficiency by considering the operating frequency and conductivity of the medium. Liu et al. [14] presented an eddy current loss analysis method in an underwater WPT system and built a coil mutual inductance model with the eddy current loss. The finite simulation and experiment they have conducted proved the effectiveness of the model and method. Liu et al. [15] established an electromagnetic field model of the underwater coil based on the non-axisymmetric model, and developed an analysis method for eddy current loss. Yan et al. [16] analyzed the eddy current loss in seawater under different misalignments and frequencies. The energy transmission efficiency is relatively unchanged under a small lateral misalignment and decreased sharply when the lateral misalignment kept growing.

However, reducing the eddy current loss of underwater WPT system using current control has not been widely studied. The researchers mentioned above reduced the eddy current loss of underwater wireless power transmission by changing the frequency of the AC power supply, the number of turns of the coil, or the structure of the coil. These methods will change the coordination and matching of the entire system. However, the method of reducing eddy current loss using current control, as proposed in this paper, only changes the parameters of the components in the compensation circuit, and does not change the characteristics of the system itself, so it is more convenient to operate and implement. In this article, the circuit of the WPT system in the air and sea is modeled sequentially, and the parameter changes caused by the eddy current loss of the seawater are analyzed. The methods of reducing eddy current loss using current control are obtained from the theoretical solutions given by past research. Increasing the current phase difference and changing the current modulus ratio in the coil can reduce the eddy current loss effectively, and the optimal modulus ratio for reducing eddy current loss is obtained through theoretical calculations. In this paper, the planar dual-coil WPT system is taken as an example, the Figure 1 shows the physical diagram and coil diagram of the planar dual-coil WPT system. And a electromagnetic field simulation of the two methods is carried out. The simulation results verify the correctness of the methods and obtain the law stipulating that the eddy current loss can be reduced by increasing the current phase.

The organization of this paper is as follows. Section 2 introduces the WPT system in the air and calculates the compensation circuit. Section 3 introduces the WPT system in the seawater and analyzes the compensation circuit, and proposes two methods to reduce the underwater eddy current loss by controlling the circuit current. In Section 4, the correctness of the two methods is verified using electromagnetic field simulation software, and the laws describing the two methods with which to reduce eddy current loss through current control are summarized in Section 5.

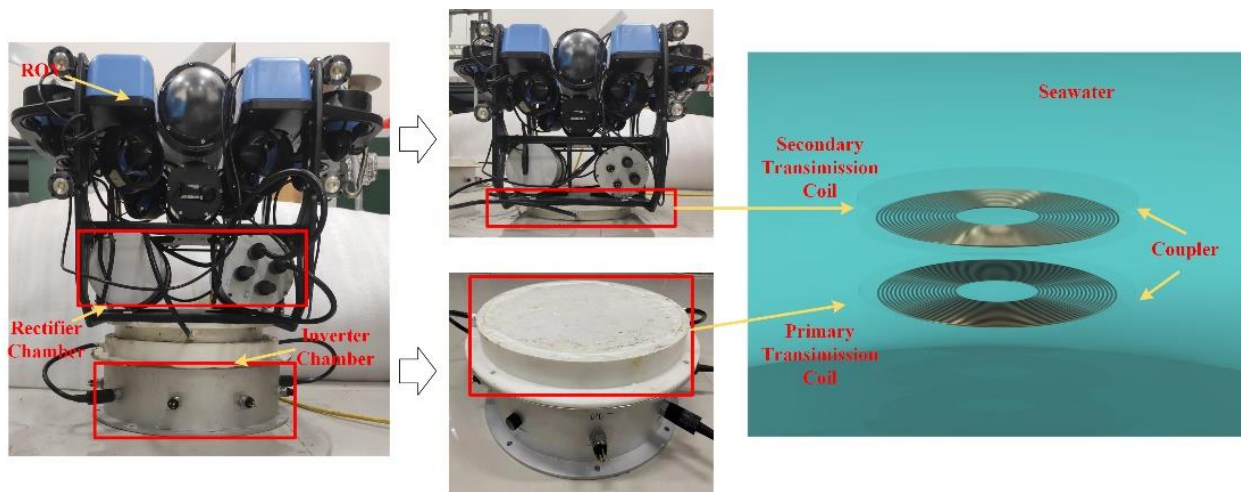


Figure 1. Schematic diagram of WPT system and planar dual-coil model.

2. Circuit Analysis in the Air

In the WPT system, the commonly used types of circuit compensation topology are series-series (SS), inductor-capacitor-inductor (LCL), double-sided inductor-capacitor-inductor (LCC-LCC), and LCC-P compensation topology. Because the LCC-LCC compensation topology has the characteristics of constant current output under the condition of constant voltage input and strong controllability, the magnitude and phase of the current in the circuits of the primary side and secondary side can be controlled by adjusting the parameters of the compensation components. Considering that this article studies the method of reducing eddy current loss using current control, the LCC-LCC compensation topology was taken as an example for analysis and research, and the equivalent circuit model in the air is shown in the Figure 2 below.

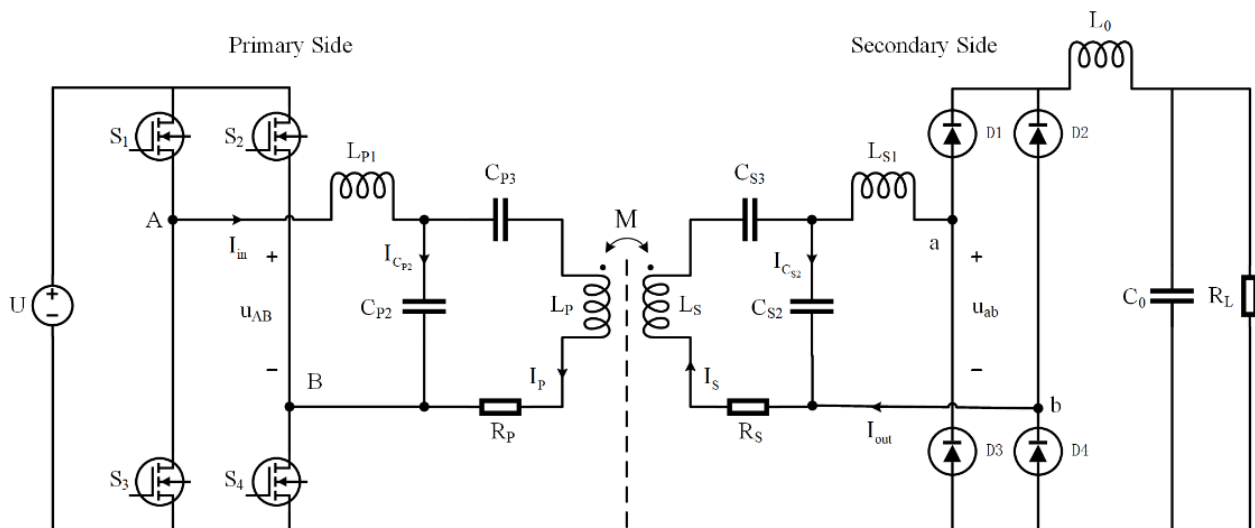


Figure 2. Double-sided LCC compensation topology for WPT system.

U is a DC power supply, and u_{AB} is the input voltage applied on the compensated coil. $S_1 \sim S_4$ are four power MOSFETs forming the inverter circuit in the primary side. u_{ab} is the output voltage before the rectifier diodes. $D_1 \sim D_4$ are four diodes forming the rectifier circuit in the secondary side. L_P and L_S are the self-inductances of the primary side coil and secondary side coil, and their internal resistances are R_P and R_S , respectively. L_{P1} , C_{P2} , and C_{P3} are the primary-side compensation inductor and capacitors. L_{S1} , C_{S2} , and C_{S3} are the secondary-side compensation inductor and capacitors, respectively. M is the mutual

inductance between two coils. L_0 and C_0 are the filter inductor and capacitor, and R_L is the load resistance. In order to facilitate the circuit analysis, we transformed the inverter circuit before point A and point B on the primary side into following form as shown in Figure 3.

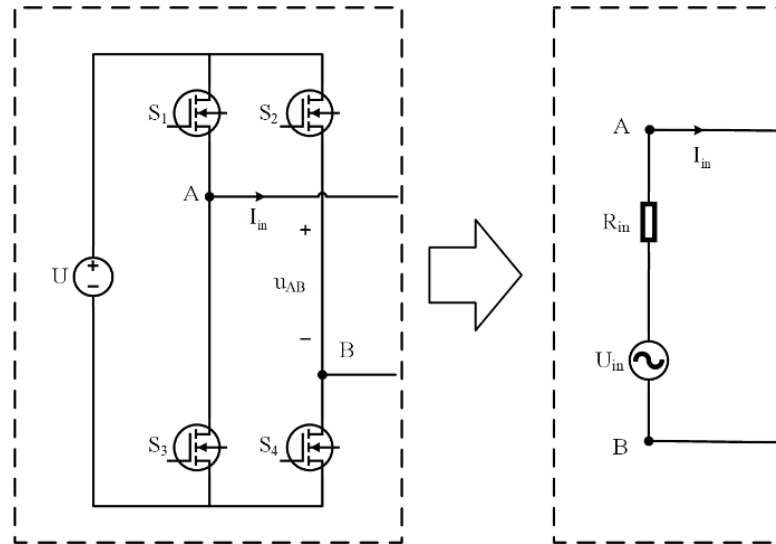


Figure 3. Equivalent circuit, focusing on the inverter circuit of the primary side.

U_{in} is the AC voltage source of U transformed by the inverter circuit, and R_{in} is the equivalent internal resistance of U_{in} . After using the same method, we obtain the equivalent circuit of the rectifier circuit after point a and point b on the secondary side in Figure 4.

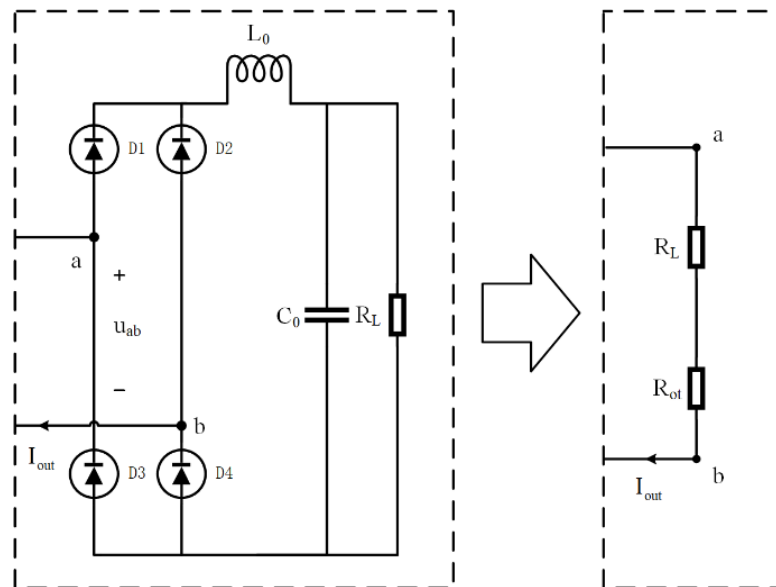


Figure 4. Equivalent circuit, focusing on the rectifier circuit of the secondary side.

The variable R_{ot} in Figure 4 represents the equivalent resistance on the conductor after converting the rectifier circuit. In Figures 2–4, I_{in} , I_{CP2} , I_P , I_{out} , I_{CS2} , and I_S are the currents going through R_{in} , C_{P2} , L_P , R_L , C_{S2} , and L_S , respectively, and they are all in phasor form.

This paper aims to study how to reduce the eddy current loss of the underwater WPT system by controlling the current on the primary-side coil and secondary-side coil without considering the influence of frequency. Therefore, in the following research process of this paper, the internal resistance of all inductors and capacitors in the compensation circuit, such as L_{P1} , C_{P2} , and L_{S1} , are neglected for the simplicity of analysis. It is also stipulated

that the phase of AC voltage source U_{in} , generated by the inverter circuit, is zero, and the frequency is f , which satisfies the following equation:

$$f = \frac{\omega}{2\pi} \tag{1}$$

The parameter ω represents the operating angular frequency of the AC current I_{in} . According to the circuit diagrams of Figures 2–4, based on Kirchhoff’s law, the equation of the primary-side circuit can be expressed as

$$\begin{bmatrix} R_{in} + j\omega L_{P1} & \frac{1}{j\omega C_{P2}} & 0 & 0 \\ 0 & \frac{1}{j\omega C_{P2}} & R_P + j\omega L_P + \frac{1}{j\omega C_{P3}} & j\omega M \end{bmatrix} \cdot \begin{bmatrix} I_{in} \\ I_{C_{P2}} \\ I_P \\ I_S \end{bmatrix} = \begin{bmatrix} U_{in} \\ 0 \end{bmatrix} \tag{2}$$

$$I_{in} = I_{C_{P2}} + I_P \tag{3}$$

Additionally, the equation of the secondary-side circuit can be expressed as

$$\begin{bmatrix} R_S + j\omega L_S + \frac{1}{j\omega C_{S3}} & \frac{1}{j\omega C_{S2}} & 0 & j\omega M \\ 0 & \frac{1}{j\omega C_{S2}} & R_L + R_{ot} + j\omega L_{S1} & 0 \end{bmatrix} \cdot \begin{bmatrix} I_S \\ I_{C_{S2}} \\ I_{out} \\ I_P \end{bmatrix} = \begin{bmatrix} 0 \\ 0 \end{bmatrix} \tag{4}$$

$$I_S = I_{C_{S2}} + I_{out} \tag{5}$$

The resonance condition of the system is satisfied by the following equations:

$$\begin{cases} j\omega_0 L_{P1} + \frac{1}{j\omega_0 C_{P2}} = 0 \\ j\omega_0 L_P + \frac{1}{j\omega_0 C_{P2}} + \frac{1}{j\omega_0 C_{P3}} = 0 \end{cases} \tag{6}$$

$$\begin{cases} j\omega_0 L_{S1} + \frac{1}{j\omega_0 C_{S2}} = 0 \\ j\omega_0 L_S + \frac{1}{j\omega_0 C_{S2}} + \frac{1}{j\omega_0 C_{S3}} = 0 \end{cases} \tag{7}$$

Equation (6) is the resonance condition of the primary-side circuit, and Equation (7) is the resonance condition of the secondary-side circuit, where ω_0 is the angular resonant frequency, which is only relevant to the inductors and capacitors in the system.

Substitute Equations (6) and (7) into Equations (2)–(5), and the total impedance of the loop on the primary side and the secondary side can be, respectively expressed as

$$Z_{in} = R_{in} + \frac{\omega_0^2 L_{P1}^2}{R_P + R_{ref}} \tag{8}$$

$$Z_S = R_S + \frac{\omega_0^2 L_{S1}}{R_L + R_{ot}} \tag{9}$$

$$R_{ref} = \frac{\omega_0^2 M^2}{Z_S} \tag{10}$$

R_{ref} is defined as the reflection impedance, which refers to the parameters that describe the impact of the secondary side on the primary side by the equivalent power method when the WPT system is working. Substitute Equations (8)–(10) into Equations (2)–(5), and the current on primary side and secondary side can be expressed as

$$I_P = -\frac{j\omega_0 L_{P1}}{R_P + R_{ref}} I_{in} \tag{11}$$

$$I_S = \frac{j\omega_0 M I_P}{Z_S} \tag{12}$$

Here, I_{in} is expressed as

$$I_{in} = \frac{U_{in}}{Z_{in}} \tag{13}$$

Additionally, we can obtain the expression of the output current:

$$I_{out} = -\frac{j\omega_0 L_{S1}}{R_L + R_{ot}} I_S \tag{14}$$

If we take I_P as the reference, I_P and I_S can be expressed as

$$\mathbf{I}_P = I_P \angle 0^\circ \tag{15}$$

$$\mathbf{I}_S = \frac{\omega_0 M}{Z_s} I_P \angle 90^\circ = \frac{\omega_0 M (R_L + R_{ot})}{R_S (R_L + R_{ot}) + \omega_0^2 L_{S1}^2} I_P \angle 90^\circ \tag{16}$$

From Equations (15) and (16), we can see \mathbf{I}_P lags \mathbf{I}_S by 90° , and the transmission efficiency of system can be calculated as

$$\eta = \frac{I_{out}^2 R_L}{I_{in} U_{in}} = \frac{\omega_0^2 L_{P1}^2}{R_{in} (R_P + R_{ref}) + \omega_0^2 L_{P1}^2} \frac{R_{ref}}{R_{ref} + R_P} \frac{\omega_0^2 L_{S1}^2}{R_S (R_L + R_{ot}) + \omega_0^2 L_{S1}^2} \frac{R_L}{R_L + R_{ot}} \tag{17}$$

It can be seen from the calculation results above that when the system works in the air environment and the compensation circuit works in the resonant state, the system has no additional loss, except the inevitable line loss of the circuit. Moreover, because the WPT system works in the resonant state, the power factor reaches the maximum and the line loss is the minimum, which indicates that the energy transmission efficiency of the system will reach the maximum at this time.

However, when the transmission system is working in an underwater environment, eddy current loss will be generated, which will cause changes in the various parameters of the transmission system and the conditions that enable the system to achieve the maximum energy transmission efficiency have changed.

3. Circuit Analysis in Seawater and Methods Proposed

In the underwater environment, due to the role of the seawater medium, not only does the electromagnetic field intensity around the coil decrease and the phase change, but the electric field intensity at the position of the coil also changes (ignoring the volume of the coil). The change in electric field intensity and phase in seawater will affect the mutual inductance, and it will cause the change in coupler impedance simultaneously [17], which will affect the working efficiency of the system. In this section, we will establish the equivalent circuit model of the underwater WPT system, and its power transmission characteristics will be analyzed so as to obtain the method to reduce eddy current loss and improve the energy transmission efficiency of the system.

According to the circuit model in the air, the underwater equivalent circuit model can be obtained as shown in Figure 5.

The difference with the air is that the self-inductance and equivalent resistance of the primary-side coil are L_{P_s} and R_{P_s} , respectively, the self-inductance and equivalent resistance of the secondary-side coil are L_{S_s} and R_{S_s} , and the mutual inductance between them is M_{sea} , which can be expressed as

$$M_{sea} = K_{sa} M_{air} e^{-j\theta_{diff}} \tag{18}$$

M_{air} represents the mutual inductance coefficient of two coils in the air, K_{sa} represents the modulus ratio of the mutual inductance coefficient between the seawater medium and air medium, and θ_{diff} represents the difference between the phase angle of the mutual inductance in the sea water medium and the air medium [18].

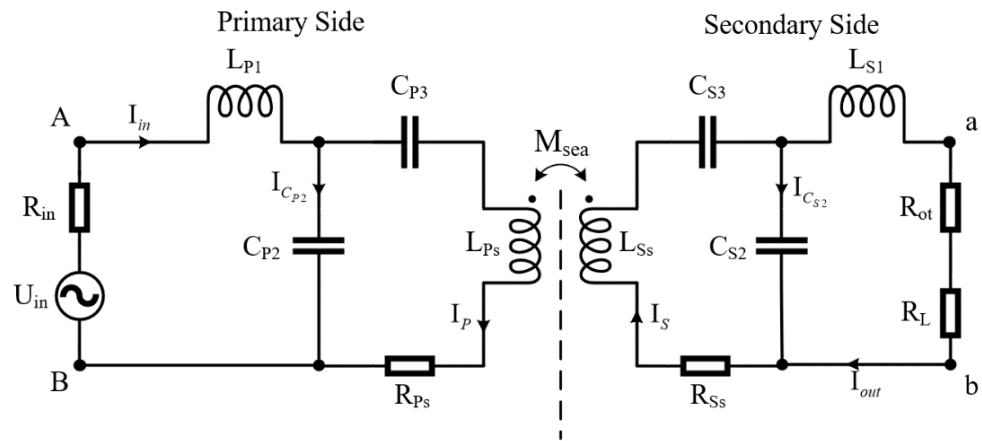


Figure 5. Double-sided LCC compensation topology for underwater WPT system.

The equivalent resistance R_{P_s} and R_{S_s} represent the sum of the resistance of the primary-side coil and the secondary-side coil and the eddy current loss resistance R_{ecl} caused by its working in the underwater environment, as shown in Equation (19). In this paper, the eddy current loss resistance is defined as

$$R_{ecl} = \frac{P_{ecl}}{I^2} \tag{19}$$

$$\begin{cases} R_{P_s} = R_P + R_{P_{ecl}} = R_P + \frac{P_{P_{ecl}}}{I_P^2} \\ R_{S_s} = R_S + R_{S_{ecl}} = R_S + \frac{P_{S_{ecl}}}{I_S^2} \end{cases} \tag{20}$$

$$P_{P_{ecl}} = \int_V \mathbf{E}_P \mathbf{J} dV = \int_V \sigma (\mathbf{E}_P^2 + \mathbf{E}_P \mathbf{E}_S) dV \tag{21}$$

$$P_{S_{ecl}} = \int_V \mathbf{E}_S \mathbf{J} dV = \int_V \sigma (\mathbf{E}_S^2 + \mathbf{E}_P \mathbf{E}_S) dV \tag{22}$$

where \mathbf{E}_P and \mathbf{E}_S are the electric field intensity and \mathbf{J} is the current density. According to Equations (19)–(22) above, it can be seen that the eddy current loss resistance is related to the electric field generated by the two coils. However, compared with the air environment, the electric field generated by the coils underwater will change. In addition, the eddy current loss resistance will also change greatly for current excitation at different frequencies. The differences between them are shown in the Figures 6–8 below.

Figures 6–8 above come from the simulation results of a single-plane coil using electromagnetic field simulation software. Figure 6 shows the AC resistance and eddy current loss resistance of the planar coil of the WPT system in the air and seawater, respectively, and Figures 7 and 8 show the comparison of its electric field intensity modulus and phase angle under different frequency excitations. It can be seen from the figure that in the air medium, the eddy current loss resistance is always zero, while in the seawater medium, with the increase in frequency, the eddy current loss resistance increases rapidly and is much larger than its own AC resistance. Moreover, from the calculation results, it can be seen that under different frequencies, the modulus of electric field intensity around the coil is almost the same in seawater and air, and the modulus in seawater is slightly less than that in air. However, it can be seen from Figure 8 that in seawater, the phase angle of electric field strength is less than 90° in air, and the farther the measurement point is from the coil, the smaller the phase angle. With the increase in frequency, the rate of phase angle reduction also increases, which shows that the emergence of eddy current loss causes the coil to produce the phase loss of the electric field.

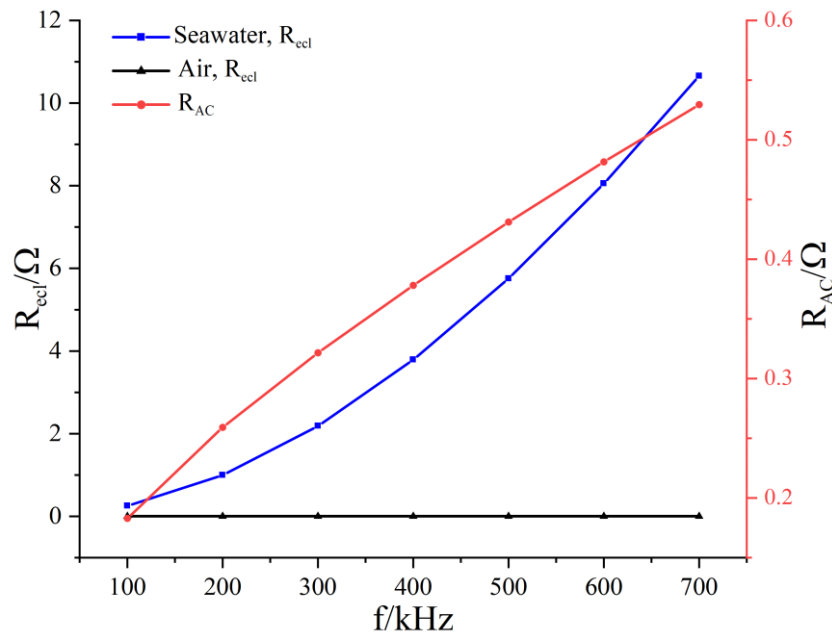


Figure 6. Variation of AC resistance and eddy current loss resistance with frequency.

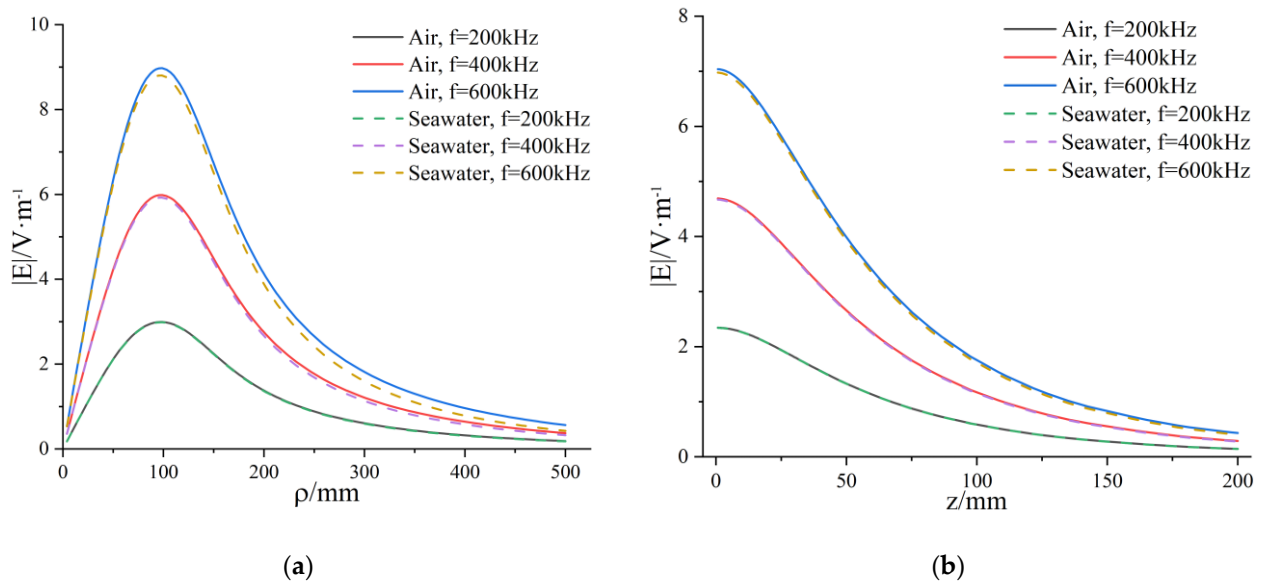


Figure 7. Modulus of electric field intensity generated by planar coil in the (a) radial direction (b) axial direction.

According to the analysis above, it should be modified appropriately when the traditional circuit model in the air is extended to an underwater environment. On the basis of Kirchhoff’s law and Figure 5, the equation of the underwater WPT system can be expressed as

$$\begin{bmatrix} R_{in} + j\omega L_{P1} & \frac{1}{j\omega C_{P2}} & 0 & 0 \\ 0 & \frac{1}{j\omega C_{P2}} & R_{P5} + j\omega L_{P5} + \frac{1}{j\omega C_{P3}} & j\omega \mathbf{M}_{sea} \end{bmatrix} \cdot \begin{bmatrix} \mathbf{I}_{in} \\ \mathbf{I}_{C_{P2}} \\ \mathbf{I}_P \\ \mathbf{I}_S \end{bmatrix} = \begin{bmatrix} \mathbf{U}_{in} \\ 0 \end{bmatrix} \quad (23)$$

$$\begin{bmatrix} R_{S_5} + j\omega L_{S_5} + \frac{1}{j\omega C_{S_3}} & \frac{1}{j\omega C_{S_2}} & 0 & j\omega M_{sea} \\ 0 & \frac{1}{j\omega C_{S_2}} & R_L + R_{ot} + j\omega L_{S_1} & 0 \end{bmatrix} \cdot \begin{bmatrix} \mathbf{I}_S \\ \mathbf{I}_{C_{S_2}} \\ \mathbf{I}_{out} \\ \mathbf{I}_P \end{bmatrix} = \begin{bmatrix} 0 \\ 0 \end{bmatrix} \quad (24)$$

$$I_{in} = I_{C_{P_2}} + I_P \quad (25)$$

$$I_S = I_{C_{S_2}} + I_{out} \quad (26)$$

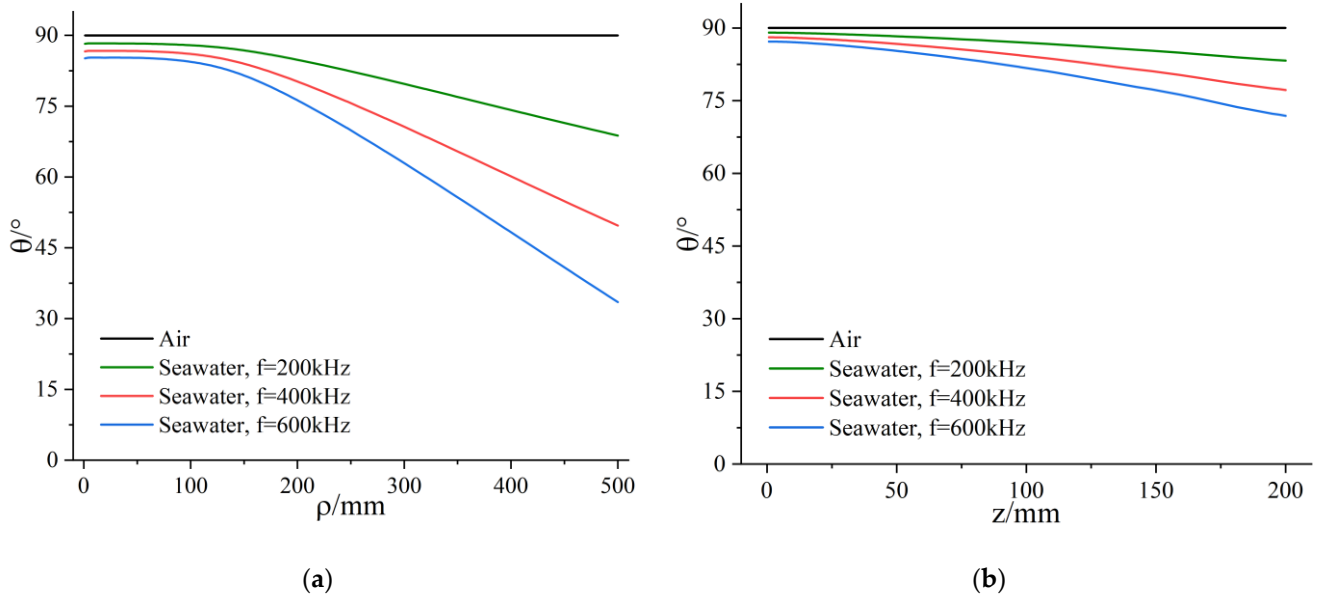


Figure 8. Phase of electric field intensity generated by planar coil in the (a) radial direction (b) axial direction.

The resonance condition on the secondary side satisfies the following equation:

$$\begin{cases} j\omega_0 L_{S_1} + \frac{1}{j\omega C_{S_2}} = 0 \\ j\omega_0 L_{S_5} + \frac{1}{j\omega C_{S_2}} + \frac{1}{j\omega C_{S_3}} = 0 \end{cases} \quad (27)$$

We can obtain the total impedance and reflection impedance at the resonance state of the primary side thusly:

$$Z_S = \frac{\omega_0^2 L_{S_1}^2}{R_{ot} + R_L} + R_{S_5} \quad (28)$$

$$\mathbf{Z}_{ref} = \frac{\omega_0^2 \mathbf{M}_{sea}^2}{Z_S} = \frac{\omega_0^2 K_{sa}^2 M_{air}^2 e^{-j(2\theta_{diff})}}{Z_S} \quad (29)$$

Due to the effect of eddy current loss, the reflection impedance of the secondary side is not purely resistive, so the resonance condition of the primary side is changed compared with that in the air. It can be obtained that the resonance condition on the primary side is

$$\begin{cases} j\omega_0 L_{P_1} + \frac{1}{j\omega_0 C_{P_2}} = 0 \\ j\omega_0 L_{P_5} + \frac{1}{j\omega_0 C_{P_2}} + \frac{1}{j\omega_0 C_{P_1}} + j\text{Im}(\mathbf{Z}_{ref}) = 0 \end{cases} \quad (30)$$

It can be calculated when both the primary side and secondary side resonate that

$$Z_P = \frac{\omega_0^2 L_{P_1}^2}{R_{P_5} + \text{Re}(\mathbf{Z}_{ref})} + R_{in} \quad (31)$$

$$\mathbf{I}_{in} = \frac{\mathbf{U}_{in}}{Z_P} \tag{32}$$

$$\mathbf{I}_P = \frac{j\omega_0 C_{P3}}{j\omega_0 C_{P3} + j\omega_0 C_{P3} - \omega_0^2 C_{P2} C_{P3} (\mathbf{Z}_{ref} + R_{P_S} + j\omega L_P)} \mathbf{I}_{in} \tag{33}$$

$$\mathbf{I}_S = \frac{j\omega_0 K_{sa} M_{air} e^{-j\theta_{diff}} (R_L + R_{ot})}{R_{S_S} (R_L + R_{ot}) - \frac{1}{\omega_0^2 C_{S2} C_{S3}}} \mathbf{I}_P \tag{34}$$

If we take I_P as the reference, I_P and I_S can be expressed as

$$\mathbf{I}_P = I_P \angle 0^\circ \tag{35}$$

$$\mathbf{I}_S = \frac{\omega_0 K_{sa} M_{air} (R_L + R_{ot})}{R_{S_S} (R_L + R_{ot}) - \frac{1}{\omega_0^2 C_{S2} C_{S3}}} I_P \angle (90^\circ + \theta_{diff}) \tag{36}$$

From Equations (35) and (36), we can infer that the phase difference between \mathbf{I}_P and \mathbf{I}_S in the seawater is not equal to 90° compared with that in the air. Additionally, from Equations (21) and (22), the eddy current loss of underwater WPT system can be expressed as

$$P_{ecl} = P_{P_{ecl}} + P_{S_{ecl}} = \int_V \sigma (|\mathbf{E}_P|^2 + |\mathbf{E}_S|^2 + 2|\mathbf{E}_P||\mathbf{E}_S| \cos(90^\circ + \theta_{diff})) dV \tag{37}$$

It can be seen that increasing the phase difference of the electric field intensity on two sides can reduce the eddy current loss when the modulus on the primary side and the secondary side is constant.

Since it is assumed that the components in the compensation topology circuit in this paper are ideal components, the resistance on the wire can be ignored because it is much less than that of the coupling coil. As a result, the energy loss of the underwater WPT system can be approximately expressed as

$$P_{loss} \approx I_P^2 (R_P + R_{R_{ecl}})^2 + I_S^2 (R_S + R_{S_{ecl}})^2 = I_P^2 R_{P_S}^2 + I_S^2 R_{S_S}^2 \tag{38}$$

Ensuring that the total output of the system remains unchanged, the total power transmitted from the primary side to the secondary side can be obtained as

$$P_t = \omega M_{sea} I_P I_S = P_{out} + I_S^2 R_{S_S}^2 \tag{39}$$

In this paper, it is assumed that the ratio of the modulus of the current in the primary and secondary coils is α , and thus we can obtain

$$I_P = \alpha I_S \tag{40}$$

$$P_{loss} = I_S^2 (\alpha^2 R_{P_S} + R_{S_S}) = \frac{\alpha^2 R_{P_S} + R_{S_S}}{\alpha \omega M_{sea} - R_{S_S}} P_{out} \tag{41}$$

The energy transmission efficiency of the system can be expressed as

$$\eta = \frac{P_{out}}{P_{out} + P_{loss}} = 1 - \frac{R_{S_S} + \alpha^2 R_{P_S}}{\alpha^2 R_{P_S} + \alpha \omega M_{sea}} \tag{42}$$

For a two-coil system with symmetrical distribution, the equivalent resistance of the primary side coil and the secondary side coil is approximately equal, and so we can obtain

$$\begin{cases} \eta = f(\alpha, \tau) = 1 - \frac{\alpha^2 + 1}{\alpha^2 + \alpha \tau} \\ \tau = \frac{\omega M_{sea}}{R_{S_S}} \end{cases} \tag{43}$$

The introduced coefficient τ is defined as the mutual inductance quality factor. When the parameters of the coils and working environment are determined, τ is a constant, and the following equations can be listed:

$$\begin{cases} \frac{\partial \eta}{\partial \alpha} = 0 \\ \frac{\partial^2 \eta}{\partial \alpha^2} < 0 \end{cases}, \alpha > 0 \tag{44}$$

Additionally, we can obtain

$$\alpha_0 = \frac{1 + \sqrt{1 + \tau^2}}{\tau} \tag{45}$$

Therefore, when the system works under the condition that the coil parameters and environmental parameters remain unchanged, changing the current modulus value of the primary side and the secondary side to make their ratio equal to α_0 can reduce the eddy current loss, which improves the energy transmission efficiency of the system.

In this section, two methods to reduce the eddy current loss of underwater WPT systems are proposed. This is realized by controlling the modulus ratio and phase difference of the current in the primary-side and secondary-side coils. Therefore, we can adjust the parameters of the components in the compensation circuit on both sides to control the current.

4. Electromagnetic Field Simulation Analysis and Discussion

In Sections 2 and 3, we analyzed the circuit model in air and seawater, and proposed two methods to reduce the eddy current loss in the underwater WPT system. In this section, we take advantage of FEA software in order to obtain the electric field intensity distribution and energy loss density distribution, and we analyze the improvement of the energy transmission efficiency of the system using two methods. For this reason, we chose to use a planar dual-coil power transmission system with symmetric distribution and establish a model as shown in the Figure 9 below, and the value of parameters in simulation are shown in Table 1.

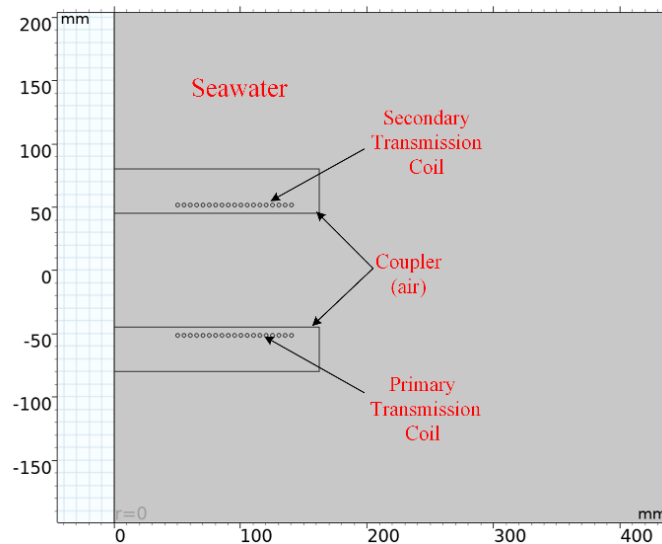


Figure 9. Simulation geometric models for underwater WPT system.

Table 1. The meanings and value of parameters in simulation.

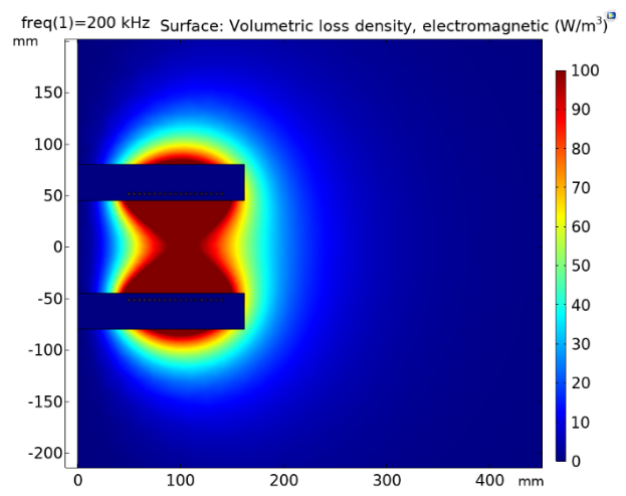
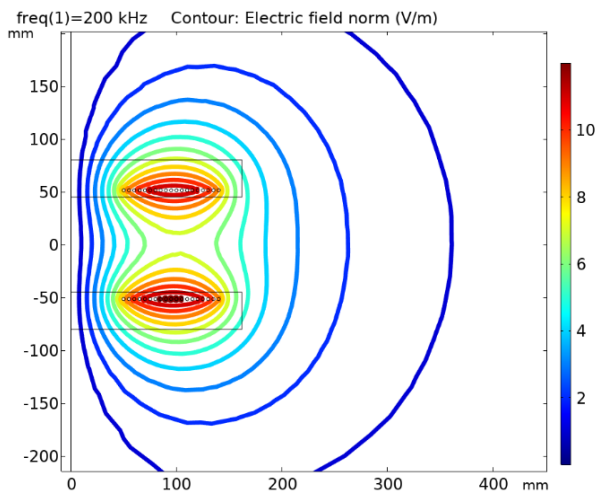
Symbol	Meaning	Value
d	Distance between two planar power transmission coils/mm	103
r	Inner radius of coil/mm	50
r_{line}	Radius of line/mm	1.5
n	Turns of coils	19
f	Frequency/kHz	200, 300
$\mu_{\text{air}}, \mu_{\text{seawater}}, \mu_{\text{copper}}$	Relative permeability for air, seawater, and copper	1, 1, 0.99990
$\sigma_{\text{air}}, \sigma_{\text{seawater}}, \sigma_{\text{copper}}$	Conductivity for air, seawater, and copper/(S/m)	0, 4.5, 5.998×10^7
$\varepsilon_{\text{air}}, \varepsilon_{\text{seawater}}, \varepsilon_{\text{copper}}$	Relative permittivity for air, seawater, and copper	1, 81, 1
R_L	Equivalent load resistance/ Ω	30
R_{ot}	Equivalent resistance of rectifier circuit and filter circuit/ Ω	0.1
R_{in}	Equivalent internal resistance/ Ω	0.2
R_P	Primary side coil resistance/ Ω	1.7
L_P	Primary side coil inductance/uH	63.45
R_S	Secondary side coil resistance/ Ω	1.7
L_S	Secondary side coil inductance/uH	64.49
M_{sea}	Mutual inductance in seawater/uH	13.31

In the simulation analysis and research below this section, under the condition of ensuring that the circuit compensation topology remains unchanged, we change the parameters of compensation components to make the power on the equivalent load resistance the definite value, and we analyze the energy transmission efficiency from primary-side AC to secondary-side AC so as to evaluate the effect of the two methods on reducing eddy current loss.

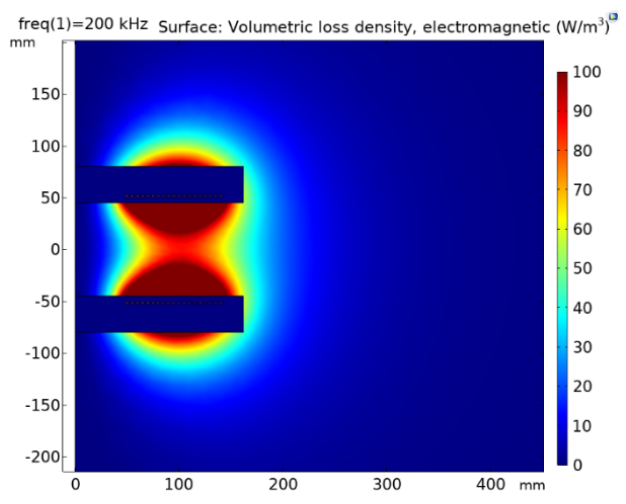
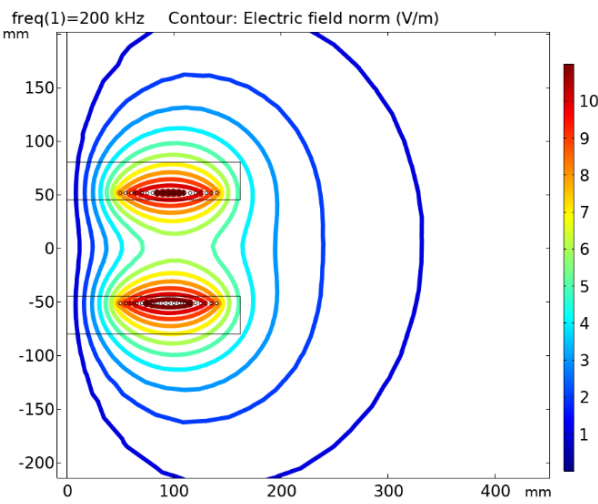
4.1. Change Current Phase Difference

Since there is no phase loss in the air medium, the phase of the field intensity excited by the coil and its current phase difference is fixed at 90° , so the phase difference of the coil excitation field strength depends on the phase difference of their current. According to Equation (37), it can be seen that increasing the field strength phase difference between the primary and secondary sides can reduce the eddy current loss; in other words, it can increase the current phase difference between the primary and secondary sides. In order to achieve this goal, there are three methods that can be adopted: the primary side resonates and the secondary side does not resonate, the primary and secondary sides do not resonate, and the secondary side resonates and the primary side does not resonate. The latter two methods will cause the current in the primary side circuit to flow back into the power supply, causing additional loss and harm to the inverter, while the primary side circuit of the first method is purely resistive and will not cause harm to the inverter. Although the secondary side circuit is not resonant, it can enter the load after current regulation and voltage stabilization, which is relatively safe as a whole. Therefore, we selected the first method in this paper.

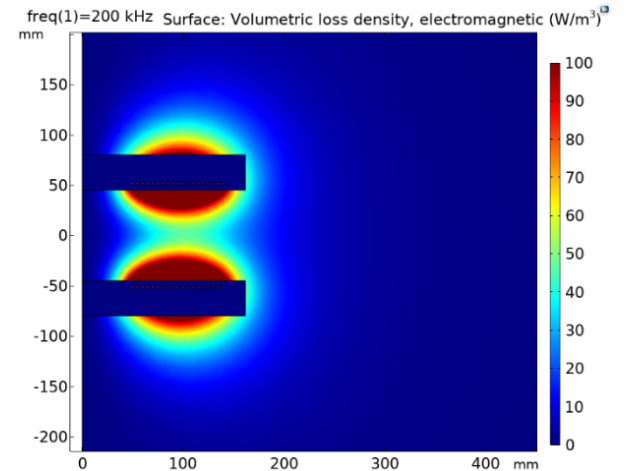
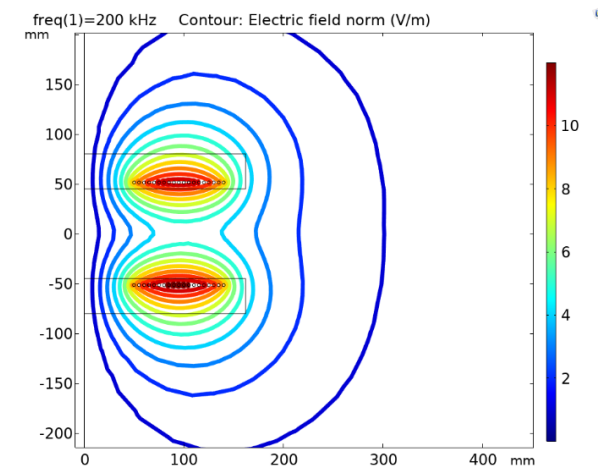
When the frequency is 200 kHz and the output current on the equivalent load resistance is equal to 1A, we change the parameters of the compensation circuit to adjust the phase difference $\Delta\varphi$ of the primary side and secondary side. We can obtain the electric field intensity distribution, energy loss density distribution, and AC-AC efficiency η , as shown in Figure 10.



(a)



(b)



(c)

Figure 10. Cont.

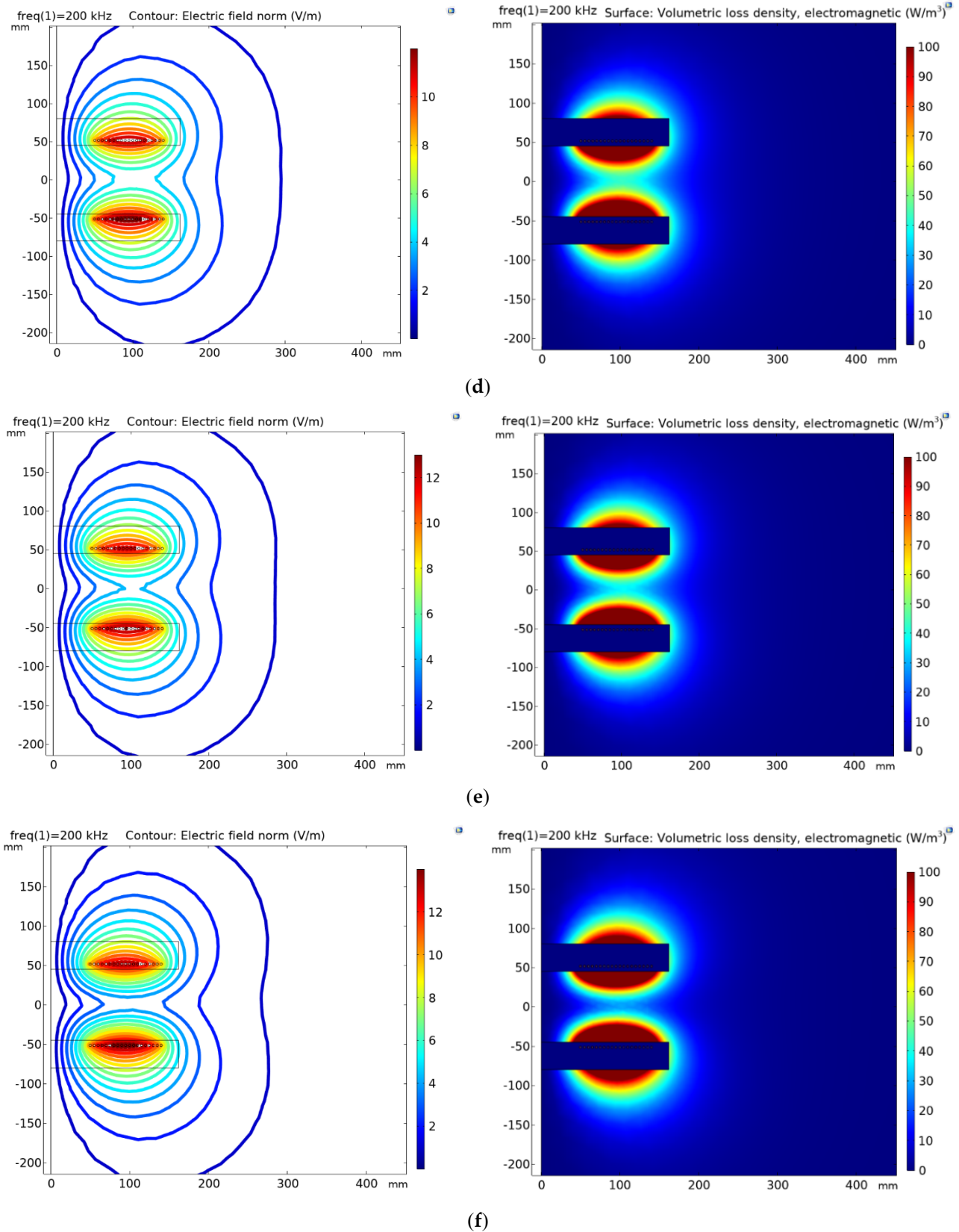


Figure 10. Electric field intensity, energy loss density, and AC-AC efficiency under different phase differences. (a) $\Delta\phi = 90.00^\circ$, $\eta = 0.8021$; (b) $\Delta\phi = 110.40^\circ$, $\eta = 0.8297$; (c) $\Delta\phi = 130.80^\circ$, $\eta = 0.8435$; (d) $\Delta\phi = 135.01^\circ$, $\eta = 0.8444$; (e) $\Delta\phi = 140.25^\circ$, $\eta = 0.8392$; (f) $\Delta\phi = 150.02^\circ$, $\eta = 0.8145$.

It can be obtained that the energy transmission efficiency of the system changes with the current phase difference, as shown in Figure 11.

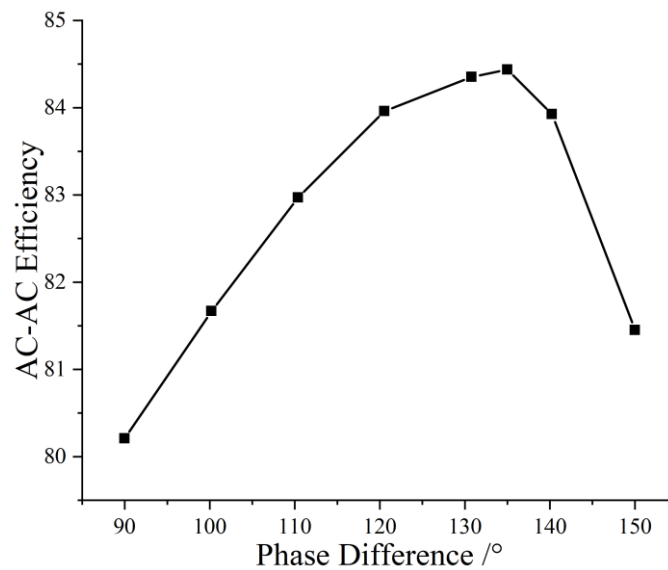


Figure 11. AC-AC efficiency varies with phase difference.

It can be seen from the simulation results that the different phases of the primary and secondary currents have little effect on the distribution of electric field strength in the area outside the coil, but it has a weakening effect on the area between the two coils. This is because the field strength outside the two coils mainly originates from the contribution of the coils themselves, while the field strength between the two coils contributes to the two coils together. With the increase in the current phase difference, the resultant field strength between the coils gradually decreases, thereby reducing the eddy current loss and improving the efficiency of the system. As shown in Figure 11, the efficiency is increased by 4.2% in the range of 90°~135°. However, as the phase difference continues to increase, the secondary side is in a non-resonant state, resulting in a decrease in power factor accordingly, and the overall efficiency of the system will decrease, as shown in the interval of 135°~150° degrees in Figure 11. Therefore, it can be seen that within a certain range, increasing the current phase difference between the primary side and the secondary side can reduce the eddy current loss and improve the energy transmission efficiency of the system.

4.2. Change the Current Modulus Ratio

According to Equation (45), for the underwater WPT systems with different resonant frequencies, there is an optimal current modulus ratio α_0 between the primary-side coil and the secondary-side coil, which can reduce the eddy current loss of the system and improve the energy transmission efficiency. In order to verify this conclusion, we kept the primary side's compensation structure unchanged, changed the parameters of the compensation components on the secondary side to control the current modulus ratio in the two coils, and then adjusted the input voltage to make the output current on the equivalent load resistance equal to 1A. The electric field intensity distribution and energy loss density distribution when the resonant frequency is at 200 kHz and 300 kHz can be obtained by means of FEA software, as shown in the Figures 12 and 13 below.

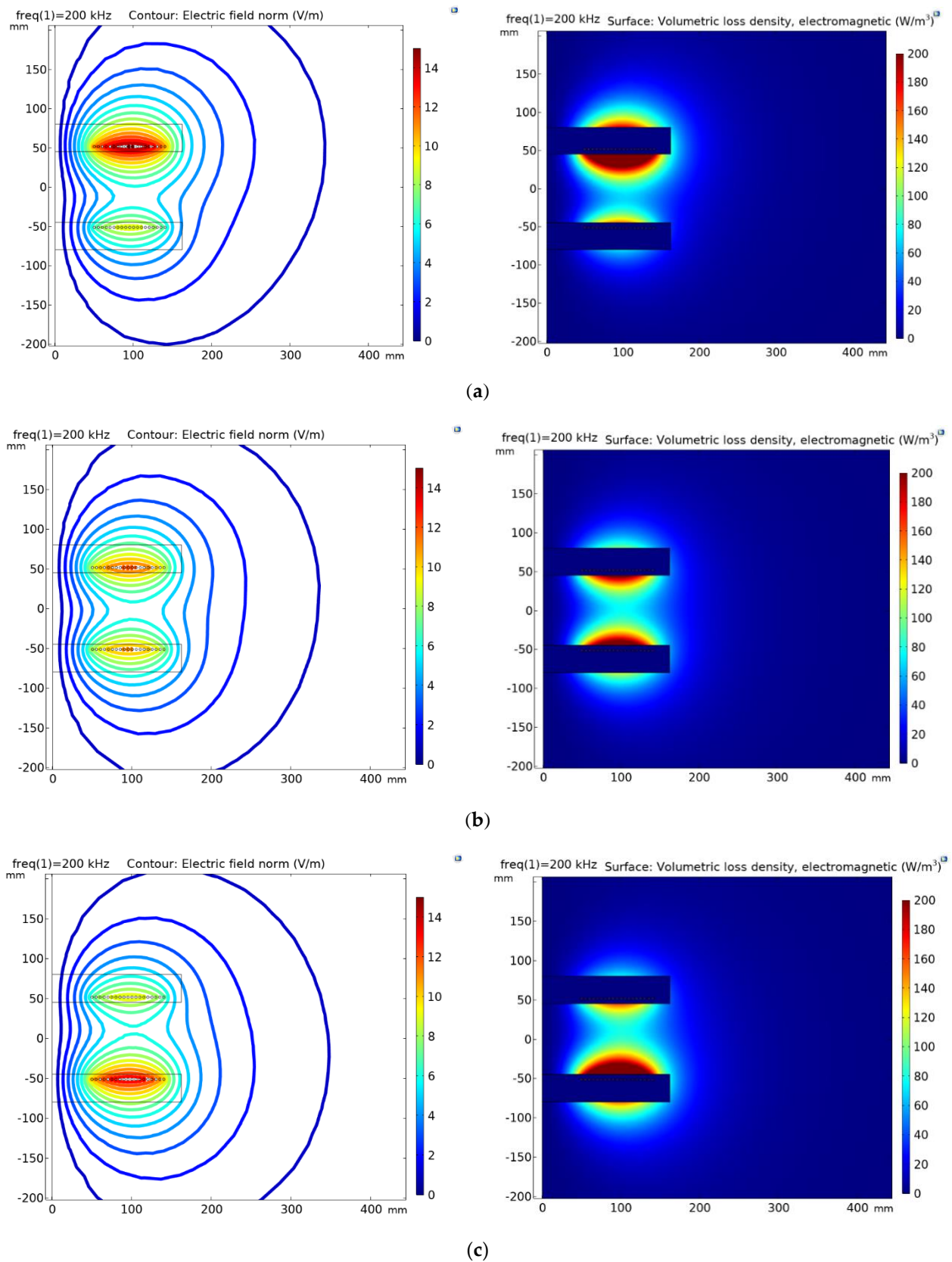


Figure 12. Electric field intensity, energy loss density, and AC-AC efficiency under different modulus ratios when $f = 200$ kHz, $\alpha_0 = 1.1068$. (a) $\alpha/\alpha_0 = 0.60$, $\eta = 0.7837$; (b) $\alpha/\alpha_0 = 0.99$, $\eta = 0.8343$; (c) $\alpha/\alpha_0 = 1.33$, $\eta = 0.8114$.

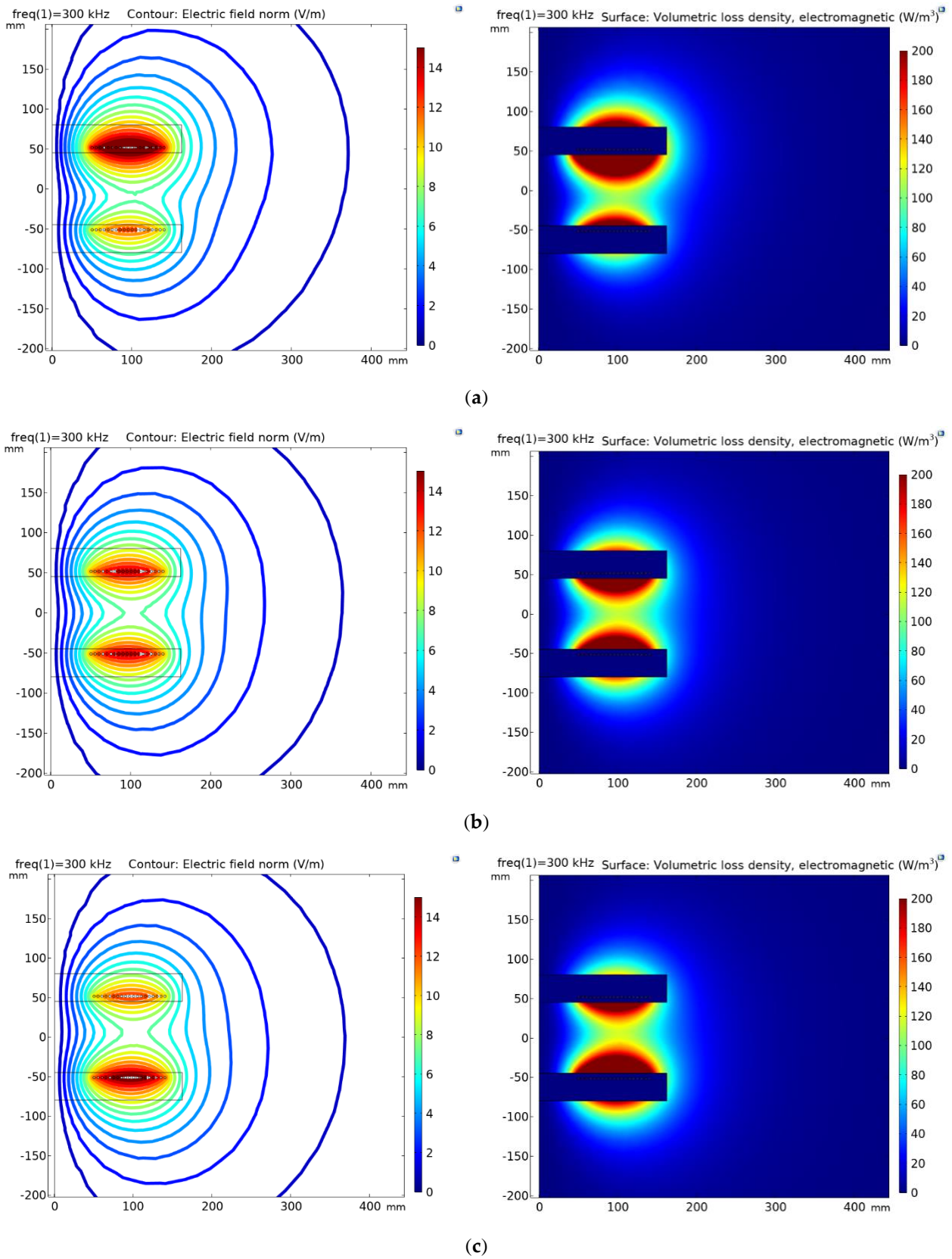


Figure 13. Electric field intensity, energy loss density, and AC-AC efficiency under different modulus ratios when $f = 300$ kHz, $\alpha_0 = 1.1103$. (a) $\alpha/\alpha_0 = 0.65$, $\eta = 0.7563$; (b) $\alpha/\alpha_0 = 1.01$, $\eta = 0.7832$; (c) $\alpha/\alpha_0 = 1.33$, $\eta = 0.8114$.

In Figures 12 and 13, α_0 represents the optimal modulus ratio calculated according to Equations (43) and (45), and α represents the modulus ratio of the current through the two coils in the simulation software. Additionally, it can be obtained that the energy transmission efficiency of the system changes with the dimensionless quantity α/α_0 , as shown in the Figure 14 below.

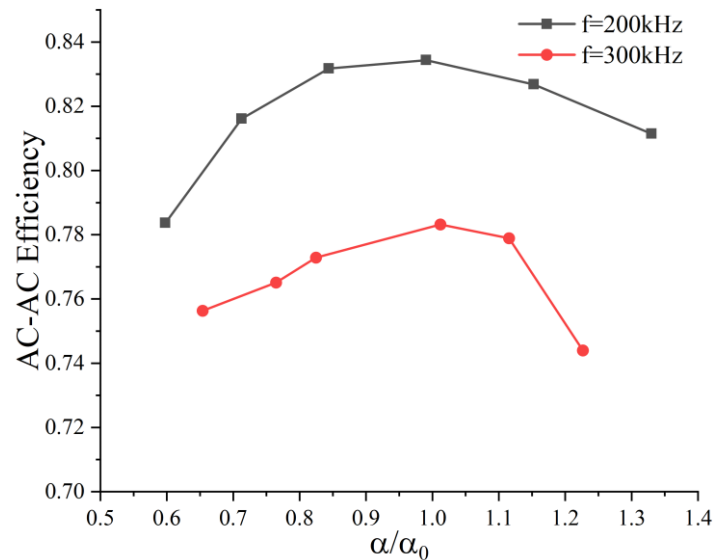


Figure 14. AC-AC efficiency varies with α/α_0 .

It can be seen from the simulation results that as the dimensionless coefficient α/α_0 deviates from 1, the asymmetry of the electric field excited by the two coils increases, and the energy loss in the area between the two coils also increases, that is, the eddy current loss increases. According to Figure 14, it can be seen that at the resonant frequencies of 200 kHz and 300 kHz, when the current modulus ratio of the two coils is equal to the optimal modulus ratio calculated by Equation (45), the energy transmission efficiency of the system is the highest, and is increased by 5.06% and 3.93%, respectively, compared with the minimum efficiency at the two frequencies. At this time, the field strength distribution around the primary and secondary side coils is evenly distributed, and the field strength maximum value in the adjacent space is small, so the energy loss due to eddy current loss is reduced, which improves the energy transmission efficiency of the system. Therefore, for a two-coil underwater wireless energy transmission system, when the modulus ratio of the current in the primary and secondary coils is controlled to ensure that it is the optimal modulus ratio, the eddy current loss of the system can be effectively reduced, and the energy transmission efficiency of the system can be improved.

5. Conclusions

In this paper, two new methods to decrease eddy current loss have been established by analyzing the circuit model of the underwater WPT system in air and seawater. It is viable to reduce the eddy current loss and improve the energy transmission efficiency of the system by controlling the current in the primary coil and the secondary coil. In addition, the underwater WPT system of planar dual coil model was established by adopting FEA software to verify the correctness of the two methods, and the simulation results are in good agreement with the calculation results. The study shows that, within a certain range, increasing the phase difference between the primary-side and the secondary-side current or adjusting the current modulus ratio of the two coils to the optimal modulus ratio can reduce the eddy current loss of the underwater system and improve the energy transmission efficiency of the system.

Author Contributions: Conceptualization, J.W. and B.S.; methodology, J.W.; software, J.W.; validation, J.W. and Y.W.; formal analysis, J.W.; investigation, J.W.; resources, J.W.; data curation, J.W.; writing—original draft preparation, J.W.; writing—review and editing, J.W., B.S., and Y.W.; visualization, J.W.; supervision, B.S.; project administration, B.S.; funding acquisition, B.S. All authors have read and agreed to the published version of the manuscript.

Funding: This research received no external funding.

Institutional Review Board Statement: Not applicable.

Informed Consent Statement: Not applicable.

Data Availability Statement: Not applicable.

Conflicts of Interest: The authors declare no conflict of interest.

Nomenclature

The following is the nomenclature of the parameters involved in this paper:

$S1\sim S4$	Primary-side MOSFETs
$D1\sim D4$	Secondary-side rectifier diodes
L_P	Self-inductance of the primary-side coil in air
L_{P1}	Primary-side compensation inductance
L_{Ps}	Self-inductance of the primary-side coil in seawater
L_0	Filter inductance
C_{P2}	Primary-side parallel compensation capacitor
C_{P3}	Primary-side series compensation capacitor
C_{S2}	Secondary-side parallel compensation capacitor
C_{S3}	Secondary-side series compensation capacitor
C_0	Filter capacitor
R_{in}	Equivalent internal resistance
R_P	Internal resistances of primary-side coil in air
R_{Ps}	Equivalent resistance of the primary-side coil in seawater
R_S	Internal resistances of secondary-side coil in air
R_{Ss}	Equivalent resistance of the secondary-side coil in seawater
R_L	Load resistance
R_{ot}	Equivalent resistance of rectifier circuit and filter circuit
R_{ecl}	Eddy current loss resistance
R_{ref}	Reflection impedance in real form
Z_{ref}	Reflection impedance in plural form
M	Mutual inductance of coils
M_{air}	Mutual inductance of coils in air
M_{sea}	Mutual inductance of coils in seawater
K_{sa}	Modulus ratio of mutual inductance coefficient between seawater and air
θ_{diff}	Phase difference of the mutual inductance between seawater and air
U	DC power supply
U_{in}	Equivalent AC power supply
I_{in}	Current on the primary-side resistance R_{in}
$I_{C_{P2}}$	Current on the primary-side compensation capacitor C_{P2}
I_P	Current on the primary-side coil
I_S	Current on the secondary-side coil
$I_{C_{S2}}$	Current on the secondary-side compensation capacitor
I_{out}	Current on the secondary-side resistance R_L

References

- Li, S.; Mi, C.C. Wireless Power Transfer for Electric Vehicle Applications. *IEEE J. Emerg. Sel. Top. Power Electron.* **2015**, *3*, 4–17.
- Li, Z.; Zhu, C.; Jiang, J.; Song, K.; Wei, G. A 3-KW Wireless Power Transfer System for Sightseeing Car Supercapacitor Charge. *IEEE Trans. Power Electron.* **2017**, *32*, 3301–3316. [[CrossRef](#)]
- Ahmad, A.; Alam, M.S.; Chabaan, R. A Comprehensive Review of Wireless Charging Technologies for Electric Vehicles. *IEEE Trans. Transp. Electrification.* **2018**, *4*, 38–63. [[CrossRef](#)]

4. Mi, C.C.; Buja, G.; Choi, S.Y.; Rim, C.T. Modern Advances in Wireless Power Transfer Systems for Roadway Powered Electric Vehicles. *IEEE Trans. Ind. Electron.* **2016**, *63*, 6533–6545. [[CrossRef](#)]
5. Zhang, K.-H.; Zhu, Z.-B.; Song, B.-W.; Xu, D.-M. A Power Distribution Model of Magnetic Resonance WPT System in Seawater. In Proceedings of the 2016 IEEE 2nd Annual Southern Power Electronics Conference (SPEC), Auckland, New Zealand, 5–8 December 2016; pp. 1–4.
6. Yan, Z.; Song, B.; Zhang, Y.; Zhang, K.; Mao, Z.; Hu, Y. A Rotation-Free Wireless Power Transfer System with Stable Output Power and Efficiency for Autonomous Underwater Vehicles. *IEEE Trans. Power Electron.* **2019**, *34*, 4005–4008. [[CrossRef](#)]
7. Kim, J.; Kim, K.; Kim, H.; Kim, D.; Park, J.; Ahn, S. An Efficient Modeling for Underwater Wireless Power Transfer Using Z-Parameters. *IEEE Trans. Electromagn. Compat.* **2019**, *61*, 2006–2014. [[CrossRef](#)]
8. Dou, Y.; Zhao, D.; Ouyang, Z.; Andersen, M.A.E. Investigation and Design of Wireless Power Transfer System for Autonomous Underwater Vehicle. In Proceedings of the 2019 IEEE Applied Power Electronics Conference and Exposition (APEC), Anaheim, CA, USA, 17–21 March 2019; pp. 3144–3150.
9. Shi, J.; Li, D.; Yang, C. Design and Analysis of an Underwater Inductive Coupling Power Transfer System for Autonomous Underwater Vehicle Docking Applications. *J. Zhejiang Univ.-Sci. C* **2014**, *15*, 51–62. [[CrossRef](#)]
10. Zhang, K.-H.; Zhu, Z.-B.; Du, L.-N.; Song, B.-W. Eddy Loss Analysis and Parameter Optimization of the WPT System in Seawater. *J. Power Electron.* **2018**, *18*, 778–788.
11. Zhang, K.; Zhang, X.; Zhu, Z.; Yan, Z.; Song, B.; Mi, C.C. A New Coil Structure to Reduce Eddy Current Loss of WPT Systems for Underwater Vehicles. *IEEE Trans. Veh. Technol.* **2019**, *68*, 245–253. [[CrossRef](#)]
12. Yan, Z.; Zhang, Y.; Kan, T.; Lu, F.; Zhang, K.; Song, B.; Mi, C.C. Frequency Optimization of a Loosely Coupled Underwater Wireless Power Transfer System Considering Eddy Current Loss. *IEEE Trans. Ind. Electron.* **2019**, *66*, 3468–3476. [[CrossRef](#)]
13. Kim, J.; Kim, H.; Kim, D.; Park, J.; Park, B.; Huh, S.; Ahn, S. Analysis of Eddy Current Loss for Wireless Power Transfer in Conductive Medium Using Z-Parameters Method. In Proceedings of the 2020 IEEE Wireless Power Transfer Conference (WPTC), Seoul, Korea, 15–19 November 2020; pp. 432–434.
14. Liu, Z.; Wang, L.; Guo, Y.; Tao, C. Eddy Current Loss Analysis of Wireless Power Transfer System for Autonomous Underwater Vehicles. In Proceedings of the 2020 IEEE PELS Workshop on Emerging Technologies: Wireless Power Transfer (WoW), Seoul, Korea, 15–19 November 2020; pp. 283–287.
15. Liu, Z.; Li, F.; Tao, C.; Li, S.; Wang, L. Design of Wireless Power Transfer System for Autonomous Underwater Vehicles Considering Seawater Eddy Current Loss. *Microsyst. Technol.* **2021**, *27*, 3783–3792. [[CrossRef](#)]
16. Yan, Z.; Song, B.; Zhang, K.; Wen, H.; Mao, Z.; Hu, Y. Eddy Current Loss Analysis of Underwater Wireless Power Transfer Systems with Misalignments. *AIP Adv.* **2018**, *8*, 101421. [[CrossRef](#)]
17. Liu, P.; Gao, T.; Mao, Z. Analysis of the Mutual Impedance of Coils Immersed in Water. *Magnetochemistry* **2021**, *7*, 113. [[CrossRef](#)]
18. Zhang, K.; Ma, Y.; Yan, Z.; Di, Z.; Song, B.; Hu, A.P. Eddy Current Loss and Detuning Effect of Seawater on Wireless Power Transfer. *IEEE J. Emerg. Sel. Top. Power Electron.* **2020**, *8*, 909–917. [[CrossRef](#)]